

ROADMAP FOR CRASHWORTHINESS FINITE ELEMENT SIMULATION OF ROADSIDE SAFETY STRUCTURES

Ala Tabiei¹ and Jin Wu²

CENTER OF EXCELLENCE IN DYNASD ANALYSIS
Department of Aerospace Eng. & Eng. Mechanics
University of Cincinnati, Cincinnati, OH 45221-0070
www.ase.uc.edu/~atabiei

ABSTRACT: The subject of this investigation is the development of an accurate simulation of a truck impacting a strong-post w-beam guardrail. Detailed methods for system simulation are proposed and three major issues which involve the use of springs to simulate component crashworthiness behavior is investigated. Rail to blockout bolt connection, soil-post dynamic interaction, and effect of ends of guardrail are modeled and simulated. Soil-post interaction is modeled using both Lagrangian and Eulerian meshes and results using the two methods are presented. The present paper provides a roadmap for simulation of highway safety structures.

INTRODUCTION

In recent years, since the number of vehicles on the roads and the roadside obstacles continues to increase, roadway systems analysis and design remains a primary goal of the FHWA. Most of the emphasis has been on conducting full-scale tests in order to gain insight into potential safety problems and to develop new and improved roadside hardware. The design of such roadside hardware as guardrails, roadway signs and light poles under vehicle impact are performed experimentally through an iterative process of design, build, test, redesign and retest, until the product meets its design criteria. The vehicle fleet have evolved. Automobiles in use today

¹ Director

² Graduate Research Assistant

cover a wider range of sizes and shapes than ever before and there is a need to use different materials for certain parts of roadside hardware. As a result, many of the factors used in the design of highway safety structures should now be reconsidered. It is economically impossible to perform full-scale field testing on a wide range of parameters. Impact simulation utilizing nonlinear FE analysis is thus rapidly becoming an effective tool in designing and evaluating these systems.

The main objective of the study is to define a finite element model that can accurately represent full-scale crash tests of the G4(1S) strong post guardrail as required by NCHRP Report 350 [1]. In the course of this approach finite element models will emerge that simulate the full-scale test data within an allowable margin of accuracy. This approach will enable us to identify the crash sensitive components of the G4(1S) guardrail safety structure under investigation. Identification of the sensitive parameters can be used as feed back in an optimization process to design new and improved guardrail system that will eliminate truck rollover. Once we are successful in validating one or more finite element models to represent full-scale crash tests, we have reached the point where the finite element simulation can be applied to new crash scenarios. Changing crash parameters, like critical angle of impact and vehicle speed, or the original design of the roadside safety structure will lead to an optimization process of the design of the roadside structure itself.

In the impact simulation using the full FE model three major issues are important when modeling the G4(1S) strong post guardrail. They are listed as follows:

1. Rail to blockout bolt connection.
2. Soil-post dynamic interaction.
3. Effect of ends of guardrail.

These issues will be treated in detail in separate sections below to propose a series of approaches for simulation.

RESEARCH METHODOLOGY AND APPROACH

Finite Element Model

The finite element (FE) model of the G4(1S) strong post guardrail system is developed using the preprocessor HyperMesh [2]. The FE model (approximately 10,000 elements) of the C-2500 pickup truck is imported into the guardrail model to generate a full FE system model. Figure 1 shows the full FE model of the system (nearly 34,500 elements). This full model is used to simulate the crashworthiness behavior of the guardrail system for evaluation of the NCHRP Report 350 for the 2000-kg pickup truck

recommendations. Specific details and dimensions for the G4(1S) guardrail system are obtained from reference [3].

Simulation of Bolt Connection

The W-beam is connected to the blockout with one bolt through a slotted hole. In the experimental testing of the guardrail system it is observed that some bolt connections are subjected to very high forces that cause the bolts to shear through and the W-beam to loss connection to the blockouts. This behavior is very important for accurate simulation of the impact event and drastically influences the redirection of the vehicle. Two different methods are available to simulate this bolt connection [4] and a third is proposed in this investigation (which is more accurate):

(i) Merging Nodes: The connection of W-beam to the blockouts is modeled by merging the nodes of the two parts. However, this method does not accurately represent the behavior of the connections, especially if the bolts become highly stressed, thus causing the possibility of breakage or pull-out of the bolts during the simulation.

(ii) Using Tied Node Sets With Failure: The connection is modeled by using the “Tied Node Sets With Failure” option in LS-DYNA3D. The tied nodes will remain connected until an average failure strain is reached in the materials of connected parts. Obviously, this method does not allow any separation of the nodes until failure has occurred. In the actual bolt connection, however, due to the slotted hole and elongation of the bolt, some movement and separation prior to the failure will happen.

(iii) Using Nonlinear Springs: Compared with the above methods, using nonlinear springs is a better approach to mimic the bolt connection. In this approach the nonlinear spring option is employed and the load curve for force-displacement of nonlinear springs is obtained through component simulation. A detailed model (4711 nodes and 4640 elements) of the bolted connection is developed using HyperMesh as shown in Figure 2. The sides of the W-beam portion are assumed to be simply supported and the bolt is given a transverse displacement as a function of time. The surface-to-surface contact option is applied to calculate the bolt-beam interaction. The RCFORC (resultant interface forces) option is invoked to collect these force data as a function of time and displacements. The data are filtered by the frequency of 300 Hz. This way the load curve necessary for the nonlinear spring is obtained. Since the bolt is located in an arbitrary position relative to the hole, the analysis is performed on basis of two extreme cases. Figure 3 and Figure 4 show these two extreme cases. The results indicate that the location of bolt has significant influence on the bolt-beam interaction. The prescribed transverse displacements to the end of the bolt were given at

several rates. Results indicate that the transverse rate of loading has little effect on the ultimate load carrying capacity of the bolt in this impact regime. The load curve for the nonlinear spring to substitute the bolt should be obtained from the actual location of bolt in the slot hole. However, since the location of the bolt is not known a priori the two extreme cases will be considered. The one that yields the closest to the test data will be chosen. In the load curves that represent bolt pullout there is no resistance against compression and the load value goes to zero once the bolt is completely pulled out through the W-beam. Therefore, the post and W-beam can continue to separate without any further force transfer, which is what happens in actual bolt failure.

Simulation of Soil-Post Interaction

The simulation of the soil-post interaction, which obviously plays a vital role in the response of the guardrail during an impact event, is a complex and important issue. Since it is computationally expensive to include the soil FE model in the impact analysis, an alternative method (see Figure 5) which involves the use of nonlinear springs is employed in this investigation to simulate the soil's response during loading. The post in soil can be viewed as a beam with build-in end. This means that there are three force reactions and three moment reactions at the end of the beam. For the problem in hand some reactions will be ignored as they are assumed to be much smaller than others. The soil-post interaction mainly consists of three dominant reaction components as follows:

- Soil-post interaction parallel to the W-beam guardrail (X-direction);
- Soil-post interaction vertical to the W-beam guardrail (Y-direction);
- Torsional interaction about the axis of the post (about Z-direction).

In general it can be assumed that the reactionary forces and moments consist of two distributed forces normal to the axis of the post and one distributed moment about the axis of the post. This assumption ignores any post pullout during an impact. These distributed reactions are due to the stiffness of the soil interacting with post deformation. Accordingly, the soil stiffness can be simulated using normal nonlinear axial springs and nonlinear torsional springs. The top left corner of Figure 6 shows a top view of a post with normal nonlinear axial springs K_1 and K_2 and nonlinear torsional springs K_3 . These springs are attached to a master node and in turn the master node is attached to all nodes of the cross-section through rigid bodies to transfer the load properly.

The force-deflection curves of these springs are obtained from component behavior by developing a FE model (7864 nodes and 7032 elements) of the full-scale post imbedded in soil. Figure 6 depicts the FE model of post-soil. Fifteen normal axial springs (5 for K_1 in the x-direction

and 10 for K_2 in the y-direction) and six torsional springs (K_3) are employed for each post in the full system FE model. These numbers of springs are chosen to represent the reaction distribution accurately. The load curves of these nonlinear springs are obtained through individual component simulation. For instance, to model the torsional rigidity of the soil-post a twisting angle as a function of time is applied at the upper portion of the post. The SECFORC option in LS-DYNA3D is invoked to obtain the cross-sectional moment (in the xy-plane) of post at several locations in the soil-post model. The section moments at A, B, C, ... etc. (see Figure 6) are obtained from the simulation and used to extract load curves for the nonlinear torsional springs at these locations in the full FE system model. Meanwhile, the rotation data of these cross-sectional centers can be achieved from the NODOUT file. In the same fashion lateral displacement is suddenly applied to the upper portion of the post to obtain the stiffnesses in the lateral directions. The SECFORC option is invoked, as for the case of torsional direction, to extract the load curves for the springs K_1 and K_2 . Using the above method the load curves (force vs. displacement or moment vs. rotation) are obtained. It is clear that this method does not allow the interaction between the deformation of the soil in the three directions. The stiffnesses are obtained in a de-coupled fashion. In this investigation, the material model for the soil as proposed in reference [5] is used to extract the load curves for the springs.

Crashworthiness simulation in general utilizes Lagrangian mesh and most of the explicit crash FE codes are Lagrangian. LS-DYNA3D recently has included Eulerian material models for impact simulation. In soil-structure interaction it is expected that soil material will fail and significant material is pushed and shuffled around. It is known that Lagrangian meshes become unstable once severe distortion occurs. Therefore, Lagrangian mesh for soil-post interaction could render the component simulation to extract the stiffnesses for the nonlinear springs inaccurately. For this purpose the simulation of soil-post dynamic interaction behavior is carried out based on both Lagrangian mesh and Eulerian mesh (see Figure 7).

Lagrangian Mesh

To simulate the soil-post interaction several models were considered as follows:

- Post is assumed to be merged with soil. No contact definition between the post and the soil is necessary. This method yields a stiffer behavior and therefore, not recommended.
- Post is not merged with the soil. Automatic_single_surface contact is defined between the post and the soil. Friction between the post and soil has great influence on the behavior.

- Post is not merged with the soil. Eroding contact is invoked to simulate soil failure. This method requires very dense mesh and yield incorrect results since the failed elements are removed which creates a gap between the soil and the post. This will cause the post to be pulled out with the application of negligible force in the axial direction of the post even if friction coefficient exceeds one.

The model with automatic_single_surface contact is used to extract the stiffnesses of the nonlinear springs. The material model used is *Mat_Soil_and_Foam_Failure. Figures 8-11 depicts the displacement and force data at the various locations of post in the x and y directions. The raw data were noisy because of the contact with friction definition. These data were filtered at 30 Hz. From figures 8 and 10, we can observe that the deflection of central nodes of post descends to negative value as the depth below grade increases. This indicates that there exists a static point of inflexion above which the deflection is positive. The nonlinear springs are placed above that point to simulate the soil-post interaction. The proper constraint is imposed on this point of inflexion. In this manner there would be not be a need to model the soil-post interaction below this point. The loads for definition of springs are taken as the difference between two adjacent cross-section forces. Figures 9 and 11 depict the cross section force vs. time data used for definition of springs in the x and y directions. For instance, to define the nonlinear spring K_1 at grade, curve A in Figure 8 is used for the displacement data, and the corresponding load data are obtained from the difference between curve A and B in Figure 9. Figure 12 depicts the load curves for nonlinear springs (K_1 and K_2) at grade in x and y directions.

Figure 7 (the one on the left) depicts the post in the soil at 100 ms. It can be observed that the mesh of the soil in the vicinity of the lower portion of the post has been severely distorted. This in general would yield dubious results. To correct such severe mesh distortions rezoning is necessary. However rezoning is a complicated and cumbersome task. Therefore, in these situations Eulerian mesh can significantly simplifies analysis and simulation of such problems.

Eulerian Mesh

Figure 7 (the one on the right) depict the post-soil interaction at 0.1 second. It is clear that mesh distortion is not an issue here because of the Eulerian formulation. The formulation allows material transfer and therefore, soil material can be pushed around with no mesh distortion. The material model used here is the same as in the Lagrangian mesh (*Mat_Soil_and_Foam_Failure) with the same values of material constants.

In using the Eulerian formulation there is no need to define contact surfaces between the post (which is a Lagrangian mesh) and the soil (which

is an Eulerian mesh). Interactions between the two materials occur through the viscous stresses. Because no contact surface with friction is defined the data for the cross sectional forces are much smoother than in the case of Lagrangian mesh. These data have been filtered with the same frequency of 30 Hz as in the case of Lagrangian mesh even though the data is very smooth. Figure 14 and 16 depict the cross sectional forces for both the x and y directions. Figures 13 and 15 depicts the displacement data at the various locations of post in the x and y directions.

Comparing the two mesh formulations it is apparent that Eulerian mesh yield much stable behavior at high material deformation. From these results it can be observed that there is some difference in the behavior even though the same material model with same material constants is used for the soil. For the behavior in the y direction the Eulerian mesh predicted higher cross sectional forces and lower displacement (see figures 11 and 16). The prediction of the two meshes for the behavior of the soil in the x direction is also different. The Eulerian mesh predicted lower displacement than the Lagrangian mesh (see Figures 8 and 13).

Simulation of End of Guardrail

The test setup for G4(1S) system [3,6] consisted of 68.6 m. Finite element model of the entire system is impractical and computationally inefficient and therefore, a simulated end effect must be included in the proposed FE model. Accurate simulation of the G4(1S) system is very much dependent on the accurate representation of the unmodeled portions. Since the W-beam redirects impacting vehicles primarily through beam tension, elastic springs are attached to the ends of the modeled W-beam to simulate its continuation in both directions. The cross section of W-beam unmodeled portion is assumed to be in the elastic range during impact and the stiffness of the spring is derived from the relationship:

$$K = \frac{EA}{L}$$

where E is the steel modulus of elasticity, A is the W-beam cross-section, and L is length of the unmodeled portion of the beam.

This approximation is investigated by developing a detailed finite element model of the unmodeled portion of the guardrail (L=25.7 m). The detailed model accounts for the effects of bolt connection and soil-post interaction. It is assumed that the effect of bolt sliding in the blockout-rail connections is insignificant. Figure 17 shows the FE model of that portion acted upon by a prescribed displacement at the front end. The SECFORC option is invoked in LS-DYNA3D to determine the cross-section forces at two locations (section AA and BB) as shown in Figure 17. The unfiltered section

forces are compared with the prediction of the above simple equation. From Figure 18 we can see a very good correlation between the simple linear spring relation and the cross-section forces obtained from the simulation of the detailed model. However, from the figure one can observe a step-wise response at low end displacement and smears out at higher displacements.

To investigate this behavior further only the guard rail, with no posts, is modeled. Prescribed end displacement is applied and the section force vs. time is depicted in Figure 18. The period of each step change is 0.01s, which coincides with the total time for a longitudinal wave to pass through this cross section from and to the point of application of the displacement. The total time can be calculated from the following formula:

$$T = \frac{2L}{\sqrt{E/\rho}}$$

Where E and ρ denote the steel modulus of elasticity and density respectively and L=25.7 m. To verify this further, Figure 18 shows the section force vs. time when the length of this rail is scaled by 0.5. Note that the period of stepwise behavior becomes half of the one before when the length of the rail is scaled by 0.5. This indicates that this phenomenon is a consequence of wave propagation. Because the effects of bolt connection and soil-post interaction are not included here the wave propagation is not damped and periodicity is apparent. However, one can observe that this periodicity is dumped out once soil-post interaction and bolt is included in the model as depicted in Figure 17.

DISCUSSION AND CONCLUSION

A detailed roadmap is presented for modeling and simulation of the G4 (1S) strong post guardrail system. This roadmap can be used for modeling and simulation of similar guardrail systems. The most important elements for crashworthiness simulation are identified and analyzed in detail. Detailed component simulation is a powerful tool for simplification of the full system model simulation. Some of the noteworthy observations are as follows:

- Approximating the stiffness of the unmodeled portions of the guardrail by a simple linear spring based on the reported equation is an acceptable simplification.
- Since position of the bolt in the slotted hole of the guardrail is random, two extreme cases are simulated and both must be used in the full model simulation to determine their effect on the total behavior.

- Both Lagrangian and Eulerian formulation is employed in the simulation of post-soil dynamic interaction. Theoretically these two methods should lead to the same results. However, there is some difference observed in the results, which is attributed to the mesh instability in the Lagrangian formulation. Eulerian mesh is more stable for soil simulation.

All the above findings will be incorporated in the full system model for crashworthiness simulation. Validation of the simulation will be carried out since test data are available. Results of the validation will be presented at later time.

Acknowledgments

Funding for this investigation is provided by the FHWA under the Center of Excellence Collaborative agreement with Mr. Martine Hargrave as contract monitor. His encouragement and the discussion with Mr. Charlie McDevitt are greatly appreciated. Computing support was provided by the Ohio Supercomputer Center. Their support is gratefully acknowledged.

REFERENCES

1. Ross, Jr., H.E., D.L. Sicking, R.A. Zimmer, and J.D. Michie. 1993. NCHRP Report 350, *Recommended Procedures For The Safety Performance Evaluation of Highway Features*, Transportation Research Board, Washington, D.C.
2. HyperMesh Manual Version 2.0, *Altair Engineering, Inc*, Troy, MI, 1995.
3. King K. Mak, Roger P. Bligh, and Wanda L. Menges, *Crash Testing and Evaluation of Existing Guardrail Systems*, Texas Transportation Institute, No. RF 471470, December, 1995.
4. Bart F. Hendricks, O. Sean Martin, and Jerzy W. Wekezer, *Impact Simulation of the 820C Vehicle with the G2 Guardrail*, Publication No. FHWA-RD-96-212, Federal Highway Administration, April, 1997.
5. Dale Schauer, F. Tokarz, G. Kay, A. Lee, R. Logan, E. Coffie, and M. Ray, *Preliminary Vehicle Impact Simulation Technology Advancement (Pre-VISTA)*, Publication No. FHWA -RD-96-059, Federal Highway Administration, February, 1997.
6. Tabiei, A., and Wu, J., "Vehicle Crashworthiness Simulation for Highway Safety Structures", *Proceedings of The Crashworthiness Symposium*, ASME, AMD, Vol. 225, pp. 165-173, Dallas, TX, 1997.

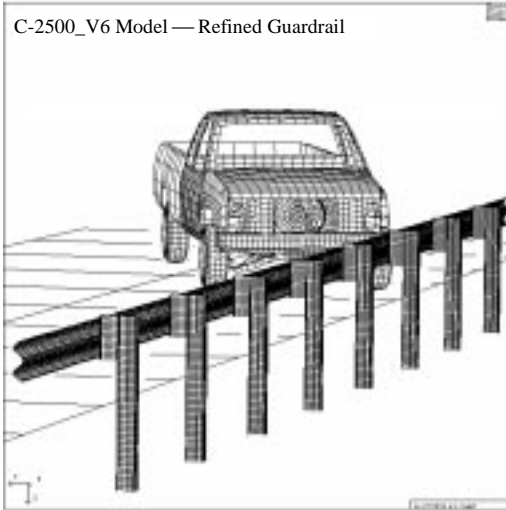


Figure 1. Vehicle and G4(1S) FE model

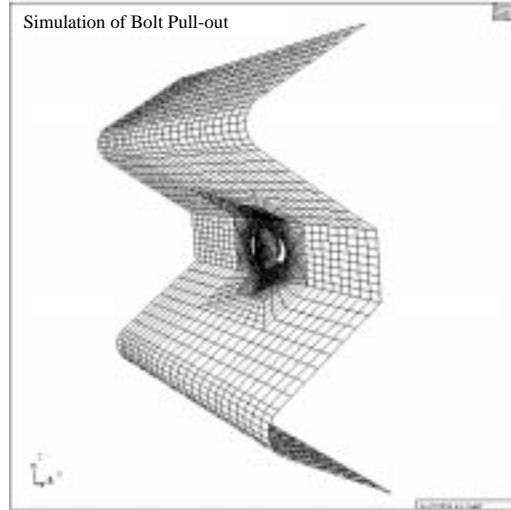


Figure 2. FE model for simulation of bolt pull-

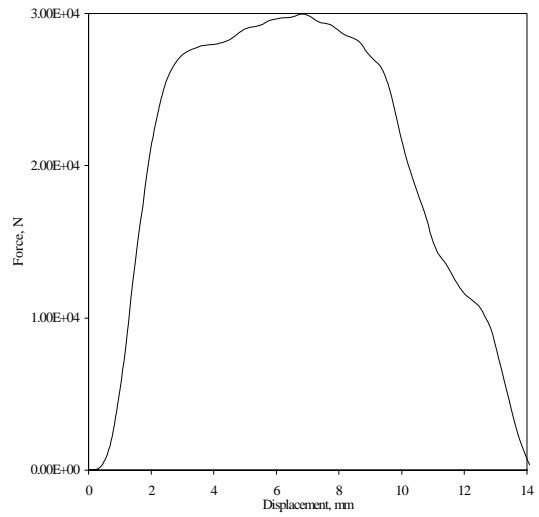
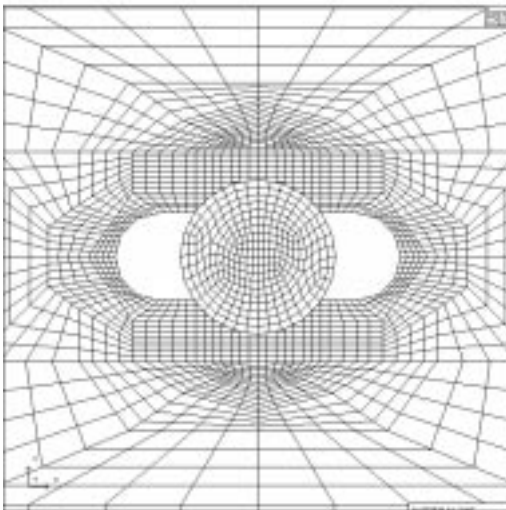


Figure 3. Simulation of bolt pull-out: (a). the bolt at the center of the hole

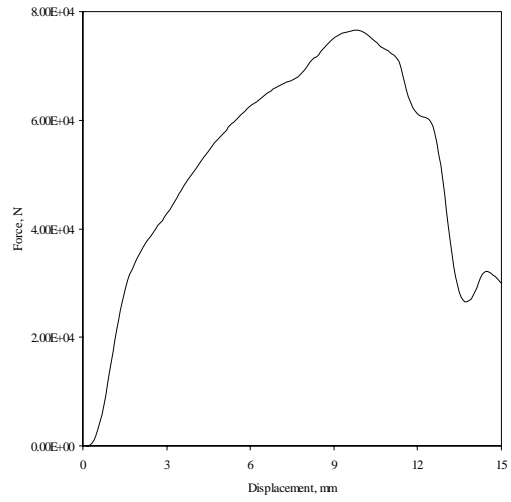
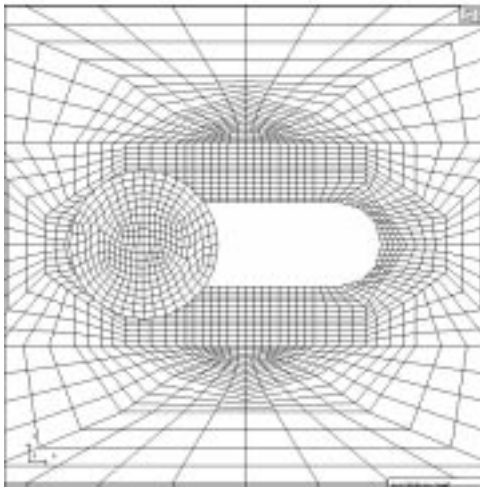


Figure 4. Simulation of bolt pull-out: (b). the bolt offset from the center of the hole

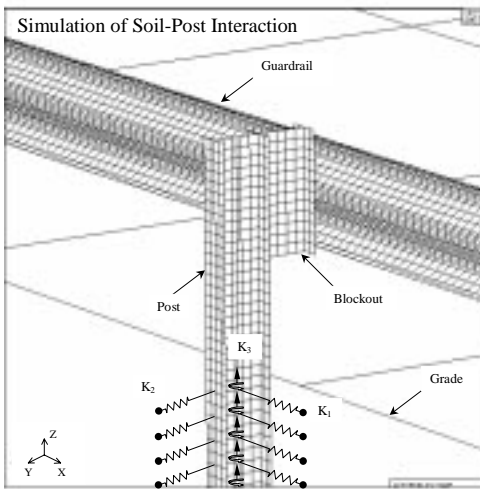


Figure 5. Simulation of soil-post interaction

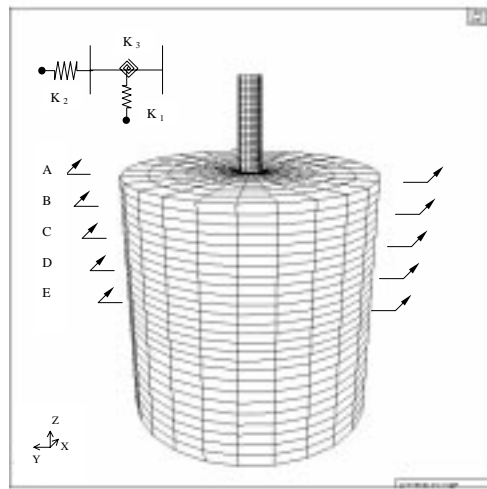


Figure 6. FE model for simulation of soil-post dynamic interaction behavior (used for Lagrangian mesh & Eulerian mesh)

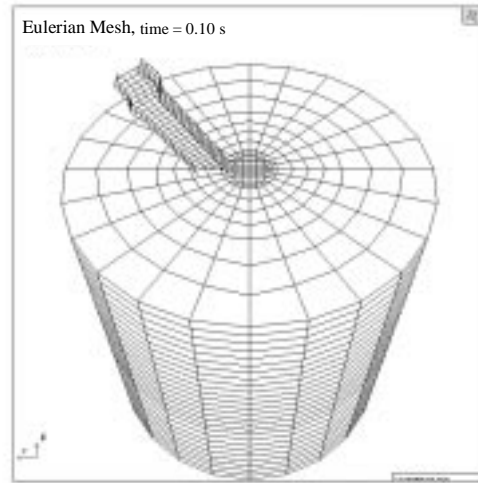
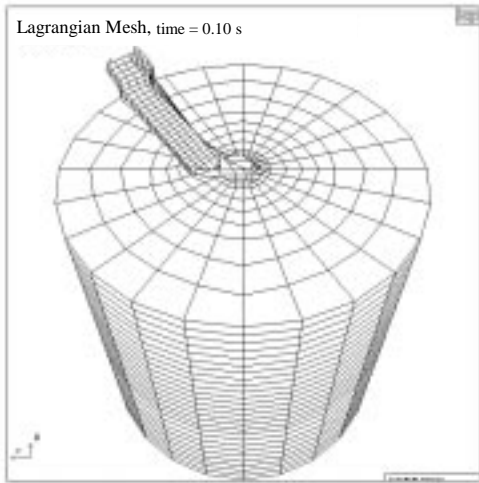


Figure 7. Soil-post interaction (Y-direction) — Lagrangian mesh & Eulerian mesh

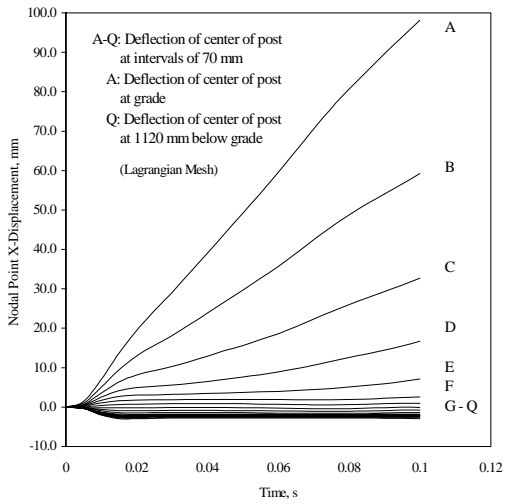


Figure 8. Nodal point x-displacement (Lagrangian Mesh)

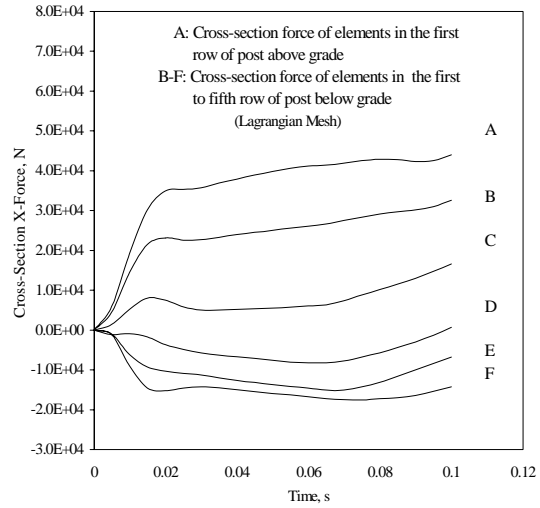


Figure 9. Cross-section x-force (Lagrangian Mesh)

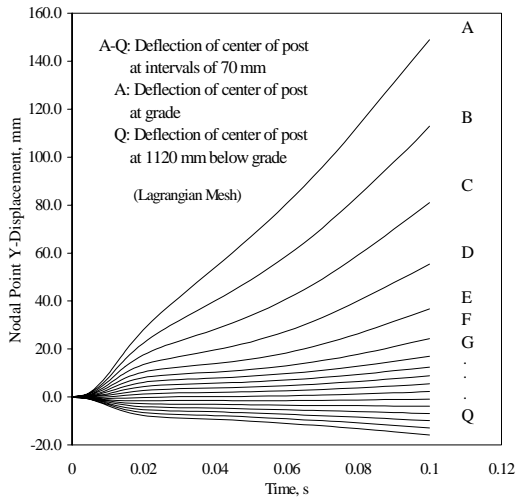


Figure 10. Nodal point y-displacement (Lagrangian Mesh)

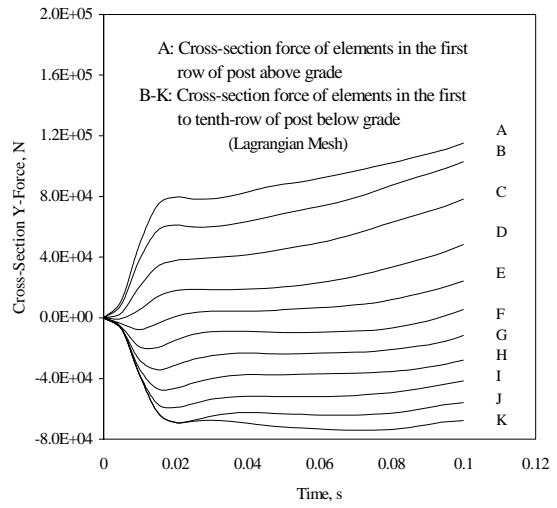


Figure 11. Cross-section y-force (Lagrangian Mesh)

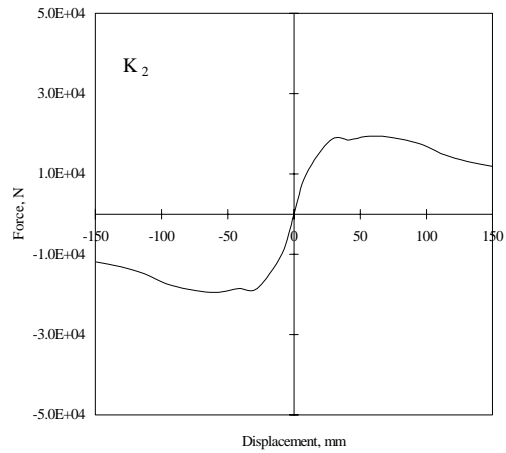
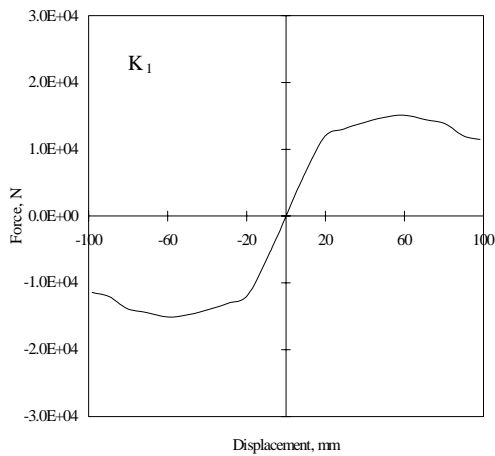


Figure 12. Load curves for the nonlinear springs (K_1 , K_2) at grade — Lagrangian

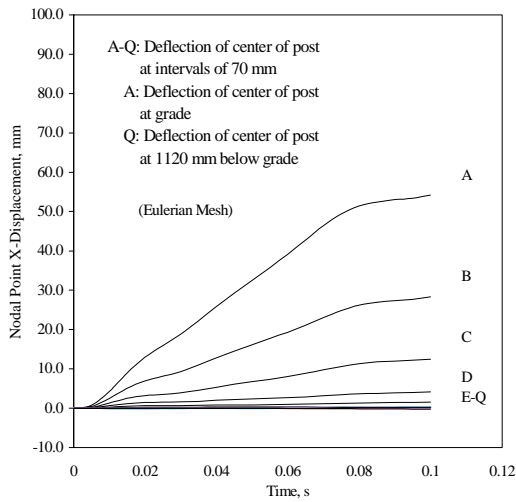


Figure 13. Nodal point x-displacement (Eulerian Mesh)

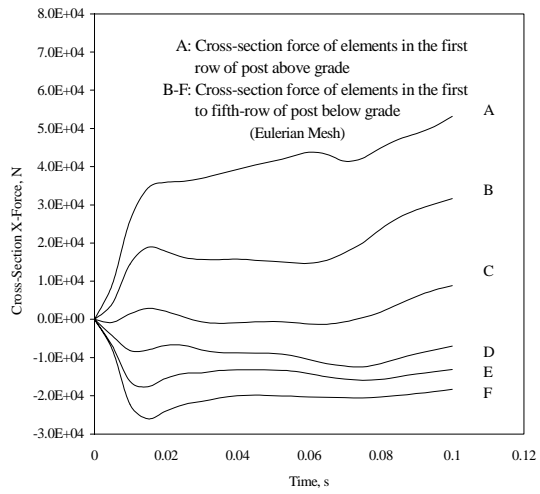


Figure 14. Cross-section x-force (Eulerian Mesh)

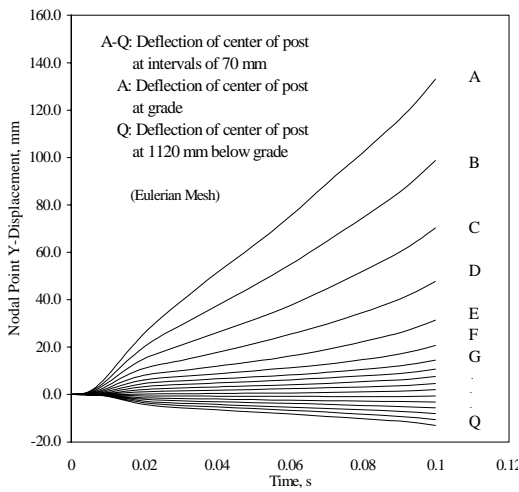


Figure 15. Nodal point y-displacement (Eulerian Mesh)

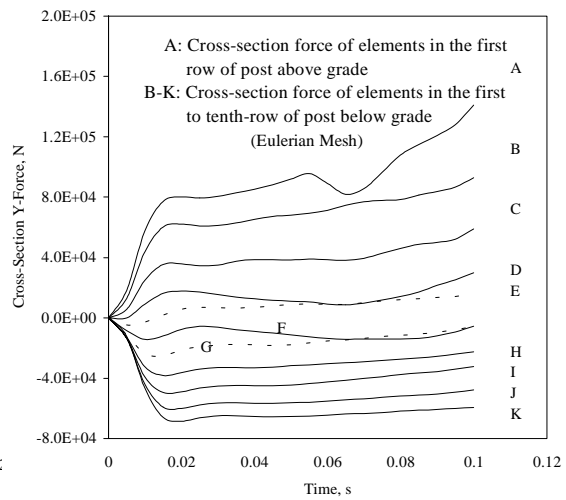


Figure 16. Cross-section y-force (Eulerian Mesh)

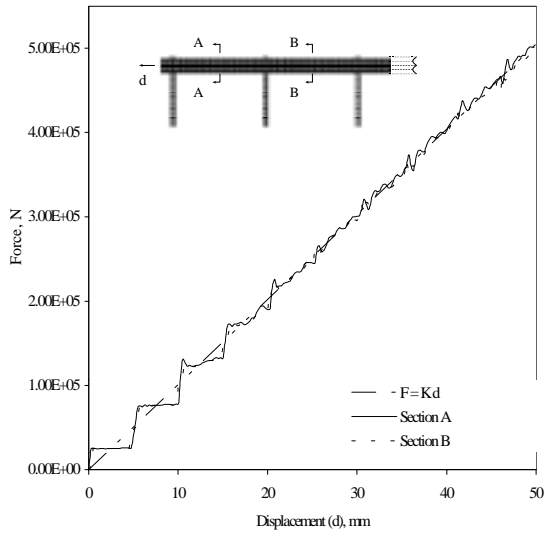


Figure 17. Simulation of guardrail extensions

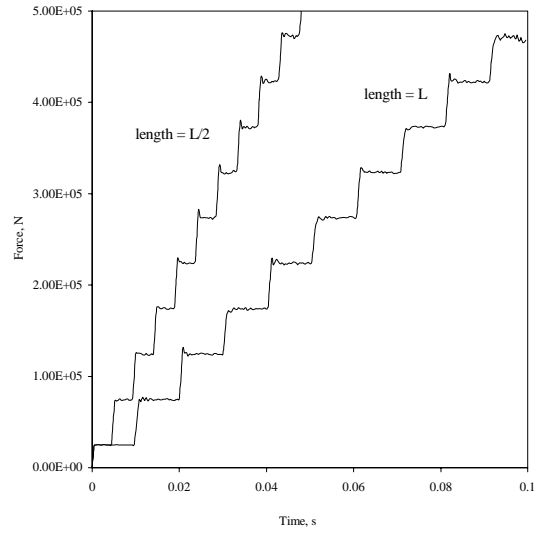


Figure 18. Simulation of beam